JOURNAL OF GEOPHYSICAL RESEARCH, VOL. 94, NO. B7, PAGES 9508–9522, JULY 10, 1989

High-Pressure Equation of State of Molten Anorthite and Diopside

SALLY M. RIGDEN,[1] THOMAS J. AHRENS, AND E. M. STOLPER

Division of Geological and Planetary Sciences, California Institute of Technology, Pasadena

New Hugoniot equation of state data for molten diopside (at 1773 K) and molten anorthite (at 1923 K) are reported to 38 and 35 GPa, respectively. The diopside data (initial density, 2.61 Mg/m^3) are described by a straight-line fit to the shock velocity-particle velocity results of $U_S = 3.30 + 1.44\ U_P$ km s^{-1}, and our preferred fit to the anorthite data (initial density, 2.55 Mg/m^3) is given by $U_S = 2.68 + 1.42\ U_P$ km s^{-1}. Reduction of the data to a third-order Birch-Murnaghan isentrope assuming the Gruneisen ratio times the density is a constant, and the Mie-Gruneisen equation of state gives K_{0S} = 22.4 GPa and K'_S = 6.9 for diopside. For anorthite we calculate K_{0S} = 17.9 GPa and K'_S = 5.3. The present data for diopside are used to calculate the diopside solidus at high pressures. We expect the solidus to be shallow above $\sim$ 10 GPa, but the lack of data on the variation of either the Gruneisen parameters of the liquid and crystal or the heat capacity and thermal expansion at elevated pressures makes extrapolation of fusion curves uncertain. Solidus temperatures of 2400-2500 K and 2560-2705 K for diopside are calculated at 10 and 20 GPa, respectively. The new data are combined with those of *Rigden et al.* [1988] for the $Di_{0.64}A_{0.36}$ eutectic composition to examine the degree to which such liquids mix ideally with respect to volume up to $\sim$ 25 GPa. For the eutectic composition at 1400°C we calculate the volumes of the An and Di mix nearly ideally to 25 GPa. We find that the ratio of the partial molar volumes of the oxides in silicate melts to that of the crystal oxides at 1673 K and 1 atm is 1.0 $\pm$ 0.1 for a wide range of oxide components. For the low-pressure tetrahedrally coordinated oxides (e.g., SiO_2, Al_2O_3, Fe_2O_3) the ratio is >1.3 with respect to oxides such as stishovite, corundum, and hematite in which the cations are octahedrally coordinated by oxygens. If changes in coordination of Al and Si from tetrahedral at low pressures to octahedral at high pressures occur in melts, they do so gradually over an interval of $\sim$ 40 GPa. Although 1 atm bulk moduli for a wide compositional range of silicate melts are similar, the differences in integrated compression to mixed oxide-like high-pressure configurations are reflected mainly by variations in K_T'. K_T' is found to vary inversely with fraction of network forming initially tetrahedrally coordinated cations (e.g., Al^{3+}, Si^{4+}). Thus K_T', which may be uncertain by $\pm$1.5, is estimated to vary from $\lesssim 7$ for molten anorthite, enstatite, and diopside to $\sim$ 8 for molten ferrosilite to $\sim$ 10 for molten forsterite and to $\sim$ 11 for molten fayalite.

INTRODUCTION

Knowledge of the high-pressure density of silicate melts provides crucial insights into the structures and thermodynamics of silicate liquids, into the nature of igneous processes at depth, and in a broad sense, into the evolution of planetary mantles and crusts. Recently, there has been considerable interest in the determination of the densities of molten silicates at high pressure, both through direct experimentation and through indirect calculations based on theoretical models and phase equilibrium data [*Stolper et al.*, 1981; *Nisbet and Walker*, 1982, *Herzberg*, 1984; *Ohtani, 1984; Rigden et al.*, 1984, *Bottinga*, 1985; *Rivers*, 1985, *Herzberg*, 1987a,b, *Agee and Walker*, 1988, *Lange and Carmichael*, 1987; *Rivers and Carmichael*, 1987]. Previously, we determined experimentally the density of a model basaltic melt on the anorthite-diopside join up to 34 GPa using shock wave techniques [*Rigden et al.*, 1984, 1988] In this paper, we report the results of similar measurements on the diopside and anorthite end-members up to almost 40 GPa.

By extending our measurements to the end-members on the diopside-anorthite join, we explore the mixing properties of this petrologically important system. The determination of mixing properties on such a join is a first step to developing methods for calculating melt densities at high pressures of compositions intermediate between those that have been experimentally studied. These methods will be critical in evaluating petrogenetic models for magmas deep in the Earth's interior; such magmas probably cover a wide range of compositions, typically rich in normative clinopyroxene and plagioclase.

The compositional dependence of equation of state parameters for liquids on the anorthite-diopside join can also give insight into the influence of Al versus Si in the compression of silicate melts. In particular, the expected change from tetrahedral to octahedral coordination of Al^{3+} by oxygen [e.g., *Waff*, 1975] at significantly lower pressures than the equivalent change for Si^{4+} [*Angell et al.*, 1982, 1983, 1987; *Matsui and Kawamura*, 1980, 1984, *Matsui et al.*, 1982; *Ohtani et al.*, 1985] might manifest itself in higher low-pressure compressibilities of Al-rich melts and different density systematics with increasing pressure. Study of the variations in melt density with composition and pressure and comparison to the densities of crystalline silicates and oxides may also lead to insights into the dependence of melt structure on composition and thermodynamic state.

[1] Now at Research School of Earth Sciences, Australian National University, Canberra, A.C.T.

Paper number 89JB00155.
0148-0227/89/89JB-00155$05.00

TABLE 1. Sample Analyses and Theoretical Compositions

	Diopside		Anorthite	
	Sample[a]	Ideal	Sample	Ideal
SiO_2	55.71	55.49	43.48	43.20
Al_2O_3	-	-	36.36	36.64
MgO	16.93	18.62	0.0	0.0
CaO	26.07	25.89	20.73	20.16
Total	98.71	100.00	100.57	100.00

[a]Average of five electron microprobe analyses. Analyst, R. Heuser.

EXPERIMENTAL TECHNIQUE

Samples of diopsidic glass were prepared from MgO, $CaCO_3$, and SiO_2. These components were weighed out in appropriate proportions to make 5 g of sample and ground together in an agate mortar under alcohol for 5 hours This mixture was placed in a Pt crucible and heated in air from 1173 K to 1723 K over 2 hours in a muffle furnace to decarbonate and melt the sample; removed from the furnace quickly and quenched the glass, heated again to 1773 K under a vacuum of ~100 μm Hg for 24 hours, quenched again to glass by removing it quickly from the furnace; and immediately placed in a box furnace in air to anneal for several days at 923 K Homogeneous, bubble-free anorthitic glass [*Boslough et al.*, 1986] was obtained from Corning Glass Company (Corning, New York). The composition, $An_{99.5}Ab_{0.4}Or_{0.1}$, is close to that of pure anorthite. Average microprobe analyses of both compositions are given in Table 1 and compared with the theoretical compositions

Discs of both samples were cored from the prepared glasses and electron-beam welded into molybdenum capsules as described by *Rigden et al.* [1988]. The diopside-bearing capsules were heated to 1723 K in a muffle furnace under a nitrogen atmosphere to check the integrity of the weld Because of the high melting point of anorthite (1826 K), this procedure was not possible with the anorthite-bearing capsules Each anorthite-bearing capsule was preheated to 1926 K in the vacuum tank of the 40-mm gun prior to firing and then cooled to <673 K, and its optical image was observed on a screen mounted outside the impact tank In this step we were able to check whether the sample had leaked, indicating a faulty weld, and whether the sample had moved in its ceramic holder, a concern because of the high temperatures required for this experiment Test samples removed from the vacuum chamber after this step and cross-sectioned contained clear, bubble-free glass

Shock wave experiments to measure the density of molten diopside and anorthite at high pressures were carried out in a 40-mm propellant gun using the techniques of *Rigden et al.* [1988]. Silicate samples contained in molybdenum capsules were suspended in the impact tank of the 40-mm gun and heated by induction under a vacuum of ~100 μm Hg to temperatures ~100 K above their melting points High pressures are generated in the sample by impact of a metallic flyer plate traveling at velocities of up to 2.5 km/s Measurement of the projectile velocity and the velocity of the shock wave that is generated in the sample allows determination of the pressure-density state in the sample by application of the Rankine-Hugoniot conservation equations

RESULTS

The results of shock wave equation of state experiments on five samples of molten diopside and six samples of molten anorthite are given in Tables 2 and 3 and shown in Figures 1-4 Also shown in Figures 3 and 4 are data on anorthosite [*McQueen et al.*, 1967], anorthitic glass [*Boslough et al.*, 1986], and crystalline diopside [*Ahrens et al.*, 1966, *Svendsen and Ahrens*, 1983]. Both sets of data are plotted in the shock velocity/particle velocity (U_S–U_P) plane in Figures 1 and 2. The diopside data fall close to a straight line. The anorthite data are also nearly linear, but as discussed below, the highest pressure point may be anomalous. We note that there is no reason, a priori, to expect that these data should fall on straight lines in these

TABLE 2. Molten Diopside Hugoniot Data

Shot	Flyer Plate	Impact Velocity, km s^{-1}	Shock Velocity, km s^{-1}	Particle Velocity, km s^{-1}	Hugoniot Pressure, GPa	Calculated Hugoniot Pressure,[a] GPa	Hugoniot Density, Mg m^{-3}	Calculated Shock Temperature,[a,b] K
660	Cu	1.03 ±0.03	4.45 ±0 04	0.73 ±0.02	8.5 ±0.3	7 5	3 13 ±0.03	1882 ±57
656	Cu	1.50 ±0.03	4.76 ±0.06	1.08 ±0.03	13.3 ±0.3	13.7	3 38 ±0.03	1937 ±88
630	Cu	2.00 ±0.04	5.28 ±0.07	1.43 ±0.03	19.7 ±0.5	20 5	3.59 ±0.03	1985 ±115
658	W	2.12 ±0.04	6.19 ±0.08	1.98 ±0.05	31.8 ±0 8	30.8	3.84 ±0.04	2043 ±150
659	W	2.42 ±0.04	6.54 ±0.11	2.24 ±0.05	38.0 ±1.0	37 6	3 98 ±0.05	2076 ±170

T_O = 1773 K, ρ_O = 2.61 Mg m^{-3}.
[a] Using value of K_{OS}, K'_S, and from Table 4; experimental Hugoniot density; γ/V equals a constant, and $C_V = 3R$
[b] Uncertainty upon varying γ_O by ± 50%.

TABLE 3. Molten Anorthite Shock Data

Shot	Flyer Plate	Impact Velocity, km s^{-1}	Shock Velocity, km s^{-1}	Particle Velocity, km s^{-1}	Hugoniot Pressure, GPa	Calculated Hugoniot Pressure[a] GPa	Hugoniot Density Mg m^{-3}	Calculated Shock Temperature,[a,b] K
666	Cu	1.24 ±0.03	3.95 ±0.04	0.91 ±0.03	9.2 ±0.3	9.3	3.31 ±0.03	2028 ±55
673	Cu	1.30 ±0.02	3.93 ±0.04	0.96 ±0.02	9.6 ±0.2	10.5	3.37 ±0.03	2037 ±60
664	Cu	1.52 ±0.03	4.36 ±0.08	1.11 ±0.03	12.4 ±0.4	11.5	3.42 ±0.04	2044 ±64
665	Cu	1.80 ±0.03	4.63 ±0.05	1.32 ±0.03	15.5 ±0.3	14.5	3.56 ±0.03	2064 ±75
663	W	2.03 ±0.04	5.40 ±0.13	1.95 ±0.05	26.8 ±0.8	26.4	3.99 ±0.06	2128 ±111
672	W	2.49 ±0.03	5.76 ±0.08	2.37 ±0.03	34.9 ±0.7	38.8	4.33 ±0.05	2181 ±141

T_O = 1923 K, ρ_O = Mg m^{-3}.
[a] Using value of K_{OS}, K'_{OS}, γ_O from Table 4; experimental Hugoniot density; γ/V equals a constant and C_V=3R.
[b] Uncertainty upon varying γ_O by ± 50%.

planes, although substances obeying simple equations of state often plot in nearly linear arrays [*Ruoff*, 1967].

The Hugoniot density-pressure (ρ – P) points based on the shock wave data and smooth curves based on straight-line $U_S - U_P$ fits to the experimental data are shown in Figures 3 and 4 The data are compatible with gradual compression without large jumps in density By comparison, the anorthosite Hugoniot centered at 300 K shows a mixed phase region above ~10 GPa (Figure 4). Crystalline diopside does not show any phase changes along the Hugoniot in the pressure range of our experiments and is considerably less compressible than molten diopside as shown by the steepness of its compression curve (Figure 3)

Using the experimental data along the Hugoniot and assuming a Mie-Gruneisen equation of state, we have obtained the isentropic bulk modulus, K_{OS}, and its pressure derivative, K' , for a third-order Birch-Murnaghan equation of state by the method of least squares previously described by *Rigden et al.* [1988] Input parameters in calculating K_{OS} and K' are the Hugoniot pressures and densities, the initial density, ρ_0, and the Gruneisen parameter, γ. The 1-atm Gruneisen parameter is calculated from the following 1-atm thermodynamic quantities· α_P, the isobaric coefficient of thermal expansion, V, the molar volume, K_{OS}, the adiabatic bulk modulus, and C_P, the isobaric heat capacity It is

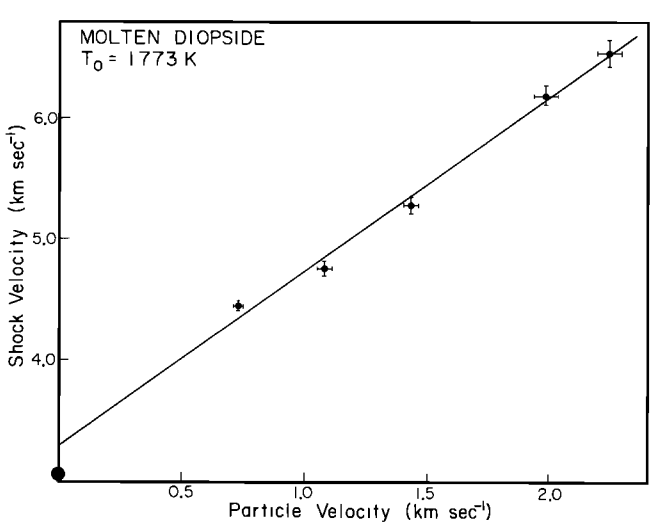

Fig. 1. Shock wave data for molten diopside (T_0 = 1773 K, ρ_0 = 2.61 Mg m^{-3}) in shock velocity (U_s)/particle velocity (U_p) plane. Straight-line fit to data are given by U_S = 3.30 + 1.44 U_P km s^{-1}, r^2 = 0.99. Solid circle at U_P = 0 is measured ultrasonic velocity at 1 atm and 1758 K [*Rivers*, 1985; *Rivers and Carmichael*, 1987].

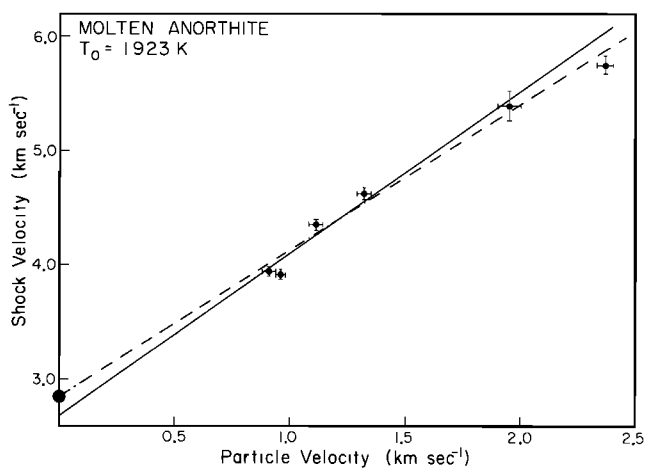

Fig. 2. Shock wave data for molten anorthite (T_0 = 1923 K, ρ_0 = 2.55 Mg m^{-3}) shown in shock velocity-particle velocity plane. Solid line is a straight-line fit to five lowest velocity data and is given by U_S = 2.68 + 1.42 U_P km s^{-1}; r^2 = 0.99. Dot-dashed straight-line fit including six data is given by U_S = 2.85 + 1.27 U_P km s^{-1}, r^2 = 0.98. Solid circle at U_P = 0 is measured ultrasonic velocity at 1 atm and 1833 K [*Rivers*, 1985; *Rivers and Carmichael*, 1987].

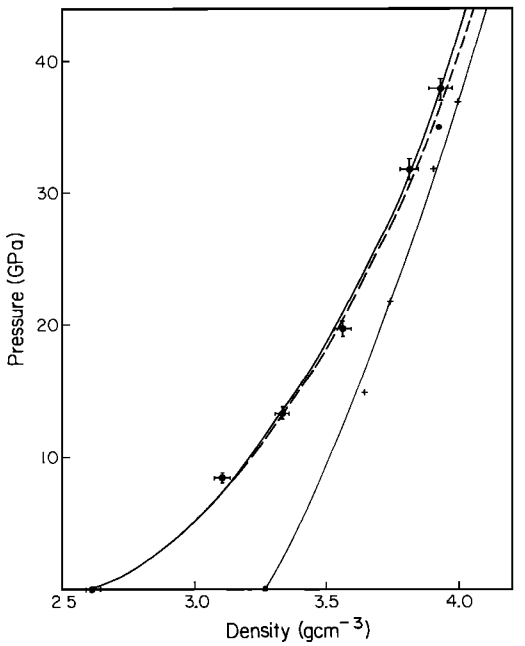

Fig. 3. Shock wave data for molten diopside (T_0 = 1773 K) in pressure-density plane. Heavy solid line is best fit to the data, and the dashed line is the best fit Birch-Murnaghan isentrope with K_{0S} = 22.4 GPa, K_S' = 6.9. Also shown are data for crystalline diopside. Solid circles are from *Svendsen and Ahrens* [1983], and crosses are from *Ahrens et al.* [1966].

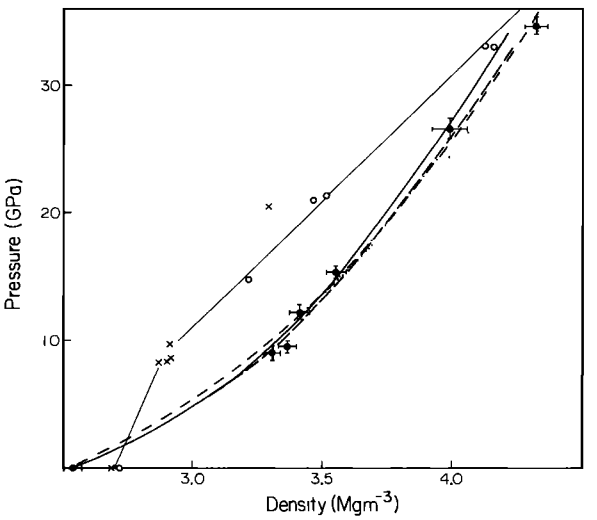

Fig. 4. Shock wave data for molten anorthite (T_0 = 1923 K) in the pressure-density plane. Heavy solid line is the best fit to the five lowest pressure data, and the dashed line is the best fit a Birch-Murnaghan isentrope with K_{0S} = 17.9 GPa, K_S' = 5.3. The best fit Hugoniot to the complete data set is given by the dash-dotted line; the accompanying isentrope (dotted line) has K_{0S} = 22.0 GPa, K_S' = 4.1. Also shown are shock wave data for anorthite glass (crosses [*Boslough et al.*, 1986]) and anorthosite (open circles [*McQueen et al.*, 1967]).

assumed, in common with *Rigden et al.* [1988], that γ/V is constant. The values of input parameters are given in Tables 2-4 and best fit values of K_{0S} and K' are given in Table 4. The calculated fit to the data is slightly better for anorthite when the five lowest pressure data are used alone (rms = 0 4 GPa compared with rms = 0 5 GPa for the complete data set) Both fits to the data are shown in Figure 4 For both molten diopside and anorthite, the values of bulk modulus calculated from our experimental data are in good agreement with the values calculated from measured ultrasonic velocities at 1 atm (Table 4). *Bottinga* [1985] determined similar values of K_{0T} and K_T' , and *Lange and Carmichael* [1987] determined a similar value of K_T' based on analysis of the fusion curve of diopside.

Shock temperatures for diopsidic and anorthitic melt are also given in Tables 2 and 3 These are calculated from the equation of state parameters of Table 4. Also given in Tables 2 and 3 are the Hugoniot pressures calculated from the experimental densities using the equation of state fit

DISCUSSION

Calculation of the Solidus of Diopside

One simple application of the equation of state of a melt with the same composition as an end-member mineral is to

TABLE 4. Input Parameters and Output for Equation of State Calculation

	Diopside	Anorthite		Units
T_0	1773	1923		K
ρ_0	2.61[a]	2.55[a]		Mg m^{-3}
α	6.0x10^{-5} [b]	3.8x10^{-5} [b]		K^{-1}
C_p	360 [a]	418 [a]		J(mol K)$^{-1}$
γ_0	0.30	0.18		
Number of points	5	5	6	
K_{0S} [c]	22.4	17.9	22.0	GPa
rms	0.4	0.4	0.5	GPa
K_S' [c]	6.9	5.3	4.1	
K_{0S}	24.2[d], 24.2[e]	20.6[d]		GPa
K_S'	5.3[e]			

[a] *Stebbins et al.* [1984].
[b] *Dane* [1941] and *Licko and Danek* [1982].
[c] This work.
[d] Ultrasonic measurement, *Rivers* [1985] and *Rivers and Carmichael* [1987]. Diopside: 1758 K. Anorthite: 1833 K.
[e] *Bottinga* [1985] from analyses of fusion curve.

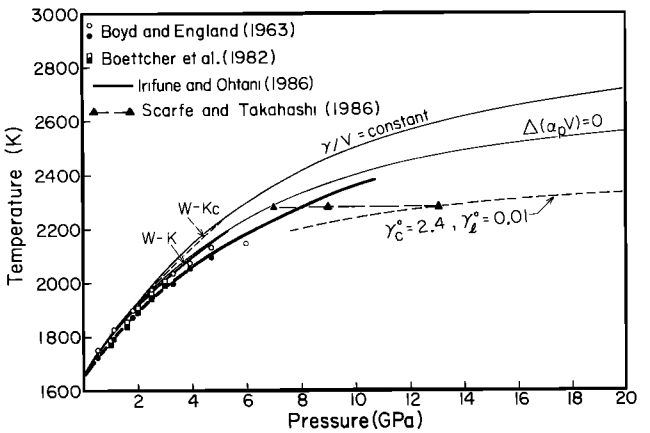

Fig. 5. Calculated fusion curve of diopside. Calculations assume γ/V is constant for both phases with preferred values given in Table 5. Lower solid curve is for thermal expansion that changes as a function of pressure. This agrees well with *Irifune and Ohtani's* [1986] data as described in the appendix. Dashed curve is also for γ/V constant but with zero-pressure values of γ_0 for the crystal (γ_c^0) and γ_0 for the liquid (γ_l^0) as indicated; these values were chosen so as to give the closest agreement with the data of *Scarfe and Takahashi* [1986]. Experimental data (open symbols are above the liquidus; solid symbols are below the liquidus) are also shown; circles, *Boyd and England* [1963]; squares, *Boettcher et al.* [1982]; *Williams and Kennedy* [1969]; W–K, data of *Williams and Kennedy* [1969]; W–K_c corrected for effect of pressure on thermocouple emf; triangles, *Scarfe and Takahashi* [1986].

the calculation of the solidus of that mineral at high pressures, providing that the mineral melts congruently Such a calculation would not be very informative in the case of anorthite because it melts congruently only at low pressures and is not stable at all above a few gigapascals [e.g., *Goldsmith,* 1980]. Diopside, although not precisely congruent in its melting behavior at 1 atm [*Biggar and O'Hara,* 1969; *Kushiro,* 1972], is an ideal candidate for such a calculation because it is stable to high temperatures and to pressures of ~ 20 GPa or more [*Liu,* 1979] and its solidus has been measured up to 13 GPa [*Boyd and England,* 1963; *Williams and Kennedy,* 1969, *Boettcher et al.,* 1982; *Irifune and Ohtani,* 1986; *Scarfe and Takahashi,* 1986].

The calculation of the solidus is in principle very simple, requiring only the integration of the Clausius-Clapeyron equation from the 1-atm melting point to the desired pressure and temperature using the thermodynamic properties (including the equations of state) of the solid and liquid phases Though simple in principle, in practice this procedure is highly dependent on the input parameters when pressure ranges of hundreds of kilobars are involved. Figure 5 shows our preferred calculation of the solidus of diopside based on our equation of state for molten diopside and selected thermodynamic properties for solid and liquid from the literature (Table 5). The details of the calculation and its extreme dependence on the input parameters (e.g., Gruneisen ratios, thermal expansion of the melt and solid versus pressure, heat capacity of melt versus pressure) are presented in the appendix.

Despite the sensitivity of the calculated solidus to the thermodynamic properties of the melt and solid phases, essentially all choices of these properties predict solidus positions compatible with experimental determinations up to 10 GPa (see Figure 5 and the appendix). In addition, using slightly different parameters for these input parameters plus our equation of state for molten diopside, *Lange and Carmichael* [1987] calculated an essentially identical fit to the solidus We thus conclude that our shock wave equation of state for diopside liquid is consistent with these phase equilibrium data. However, although the solidus most certainly flattens out above 5 GPa (i.e., $\Delta V \rightarrow 0$) as

TABLE 5. Parameters Used for Calculation of Fusion Curve of Diopside

	Crystalline Diopside	Molten Diopside	Units
T_0	1664[a]	1664	K
V_0	69.11[b]	81.09[c]	$m^3\ mol^{-1} \times 10^{-6}$
		82.34[d]	$m^3\ mol^{-1} \times 10^{-6}$
		82.95[e]	$m^3\ mol^{-1} \times 10^{-6}$
ΔS_f^0	82.88[f]		$J(mol\ K)^{-1}$
K_T	90.7[g]	21.9[h]	GPa
K_T'	4.5[g]	6.9[h]	
α	3.2×10^{-5} [i]	6.0×10^{-5} [c,e]	K^{-1}
		6.5×10^{-5} [d]	K^{-1}
		7.3×10^{-5} [j]	K^{-1}
C_p	$328.19 + 1.888 \times 10^{-3}\ T$	334.57[k]	$J(mol\ K)^{-1}$
	$-2.5192 \times 10^3 T^{1/2} - 1.443 \times 10^6 T^{-2}$ [l]		
	$243.9 + 1.069 \times 10^{-2} T$ [m]	353 [m]	$J(mol\ K)^{-1}$
γ_0	0.61	0.35	

[a] *Kushiro* [1972].
[b] Calculated using room temperature volume of *Robie et al.* [1978].
[c] *Dane* [1941].
[d] *Stebbins et al.* [1984].
[e] *Licko and Danek* [1982].
[f] *Stebbins et al.* [1983].
[g] Calculated using bulk modulus of *Levien and Prewitt* [1981] and $(dK/dT)_p$ of *Bottinga* [1985].
[h] Calculated from shock data on molten diopside and thermodynamic parameters to yield K_T at 1664 K.
[i] *Finger and Ohashi* [1976] and *Skinner* [1966].
[j] *Bottinga et al.* [1983].
[k] *Richet and Bottinga* [1984].
[l] *Bottinga* [1985].
[m] *Rivers* [1985] and *Rivers and Carmichael* [1987].

predicted by *Herzberg* [1984] and *Rigden et al.* [1984], the existence or precise position of a maximum on the diopside solidus at higher pressure cannot be predicted with confidence from our data in the absence of more reliable information on liquid compositions along the solidus, on the 1-atm volume of the melt, and on the Gruneisen ratios (or the α_P functions) of diopsidic melt and solid. The curve calculated assuming that $\Delta(\alpha_p V)$ decreases from its 1-atm value to zero at about 9 GPa (labelled $\Delta(\alpha_p V)=0$ in Figure 5) agrees closely with the determination of the solidus by *Irifune and Ohtani* [1986] to 10 GPa but lies at higher temperatures than the data of *Scarfe and Takahashi* [1986] at 13 GPa. Our equation of state parameters are only compatible with the abrupt and extraordinary flattening of the solidus at 7-13 GPa observed by *Scarfe and Takahashi* [1986] if an unrealistically low value for γ_o is chosen for the liquid (Figure 5), and for this choice of γ_o, the <5 GPa data are not readily accounted for. More data are required to resolve this apparent discrepancy.

Mixing Properties of Anorthite-Diopside Liquids

One of the most important questions in the study of silicate liquids in the composition range of interest to mineral physics and petrology is the degree to which their thermodynamic properties can be approximated by ideal mixing The nearly ideal mixing behavior of silicate melts at 1 atm with respect to volume (i.e., $\Delta V_{mix} \sim 0$) has great practical significance since it permits the accurate calculation of melt densities as a function of composition [*Bottinga and Weill,* 1970; *Nelson and Carmichael,* 1979; *Bottinga et al.,* 1982, 1983; *Stebbins et al.,* 1984; *Lange and Carmichael,* 1987]; indeed, it is on this basis that the 1-atm densities used in reducing our shock wave data were calculated. This feature also provides a basic structural insight: the local environments occupied by a particular cation in silicate melts are not greatly influenced by melt composition. In those cases where deviations from ideal behavior are detected [e.g., *Bottinga et al.,* 1983], inferences about variations in molecular level structures with composition may be drawn

In Figure 6 we show the specific volume versus pressure for molten anorthite, $An_{0.36}Di_{0.64}$, and diopside along 1673 K isotherms These curves were calculated from our shock wave data for molten diopside and anorthite (using the K_{OS} and K' values from the five-point fit to the anorthite data) and that of *Rigden et al.,* [1988] We assumed that the specific heat at constant volume is 3R and that γ/V is constant for each composition. In the inset to Figure 6 we compare the volume of the An-Di eutectic composition at 1400°C based on our shock wave measurements [*Rigden et al.,* 1988] with the volume of an ideal mixture of anorthite melt and diopside melt at the same temperature based on this work. The density of the intermediate composition can be calculated to within 1 5% up to 25 GPa based on the assumption of ideal mixing of the end-members (Figure 6). We consider this to be an impressive result, given that the compressions involved between 1 atm and 25 GPa are about 30%. If this can be shown to hold for a wider range of compositions at high pressures, it will permit the precise calculation of melt densities at elevated pressures in a simple fashion. Such a scheme for calculation of melt densities would contribute significantly to efforts to model the evolution of melts evolving at pressures on the order of tens of gigapascals Although not likely to be important in the evolution of common, modern igneous rocks, petrogenesis at these pressures may have been important early in the history of the Earth [e.g , *Stolper et al.,* 1981; *Herzberg,* 1984, *Rigden et al.,* 1984] and in the development of komatiites [*Nisbet and Walker,* 1982; *Herzberg,* 1983, *Ohtani,* 1984].

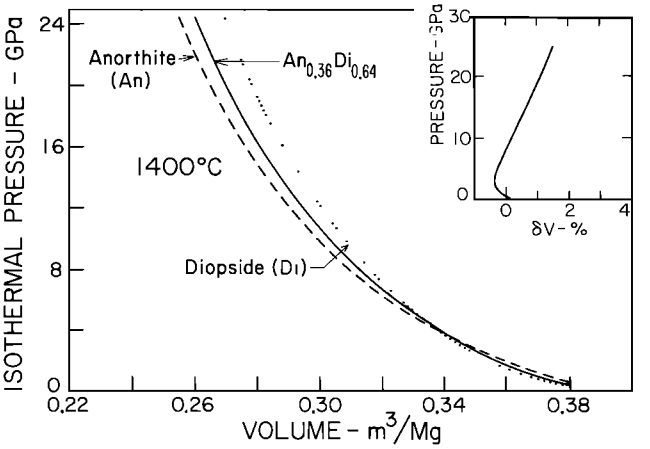

Fig. 6. Variation of volume of molten anorthite, diopside, and $An_{0.36}Di_{0.64}$ with pressure along 1673 K isotherms calculated from shock wave data. The inset shows the percent deviation of calculated volume of an ideal mixture of molten anorthite and diopside (this work) from the isothermal volume of $An_{0.36}Di_{0.64}$ (from shock wave data [*Rigden et al.,* 1984, 1988] as a function of pressure at 1673 K. $\delta V(\%) \equiv (V_m - V_T)/V_m\,(100)$, where V_m is the volume of an ideal mixture of anorthite and diopside melt corresponding in composition to the 1-atm eutectic based on this work and V_T is the volume of a melt of this composition based on the results of *Rigden et al.* [1988]. The comparison is only carried to 25 GPa because of the abrupt, unexplained stiffening observed at about this pressure for the eutectic composition.

We note that the abrupt stiffening of the eutectic composition above 25 GPa [*Rigden et al.,* 1988] is not observed in the end-members; if the behavior of the eutectic composition under shock compression above 25 GPa reflects a relaxed liquid state (as opposed to some of the alternatives discussed by *Rigden et al.* [1988]), this would indicate that the approximation of ideal mixing with respect to volume breaks down under these conditions

Structures of Silicate Melts at High Pressures

Al^{3+} and Si^{4+} coordination changes. Although density is a reflection of the integrated molecular structure of a substance, it is in general difficult to infer microscopic structural characteristics from equation of state measurements It is, however, possible to test the validity of hypothesized structures and of proposed changes with composition, pressure, and temperature by using density measurements. In this section, we examine using our data the hypothesis that compression of aluminosilicate liquids up to pressures of a few tens of gigapascals involves coordination changes of Al and Si.

As shown in Figure 7, the partial molar volumes at 1 atm of oxides (excepting Al_2O_3, Fe_2O_3, SiO_2, and TiO_2 in Na-bearing compositions) in silicate liquids over the compositional range of typical magmas are similar ($\pm$ about 10%) to the volumes of the dense, crystalline oxides. This is consistent with the hypothesis of *Gaskell* [1982] based on a study of the density systematics of alkali silicate glasses that the "network-breaking" components (e g., MgO, FeO,

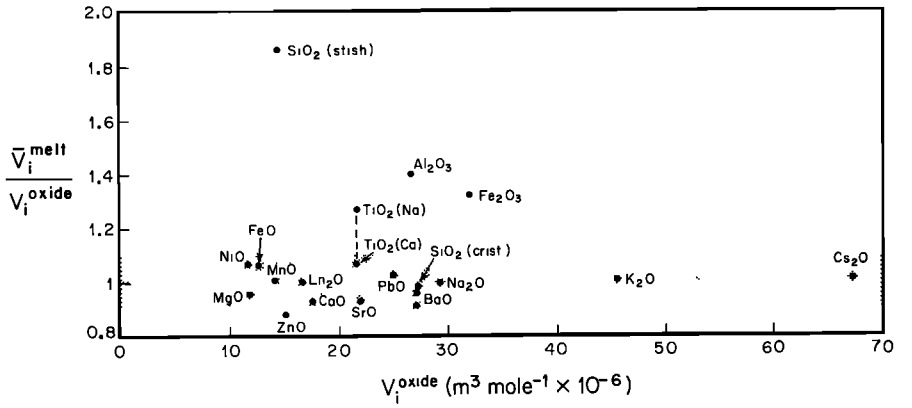

Fig. 7. The ratio of the partial molar volume in silicate melt and volume of crystalline oxide ($\bar{V}_i^m/V_i^{oxide}$) versus V_i^{oxide} at 1673 K and 1 atm. Except for Fe_2O_3, Al_2O_3, and SiO_2(stish.) (and perhaps TiO_2(Na)), where it is likely that the cation is tetrahedrally coordinated in the melt but the crystalline oxide is based octahedral coordination, $\bar{V}_i^m/V_i^{oxide}$ is between 0.9 and 1.1 over a wide range of volume. Stippled region shows a ±10% variation about $\bar{V}_i^m/V_i^{oxide} = 1.0$. Two points are plotted for TiO_2: the one labelled "Na" is based on the partial molar volume of TiO_2 in Na-bearing, Ca-free liquids; the one labelled "Ca" is based on the partial molar volume of Ca-bearing, Na-free liquids. Both of these points use anatase as the crystalline oxide. Two points are shown for SiO_2: the one labelled "stish" uses the volume of stishovite for the oxide, whereas the one labelled "crist" uses cristobalite. Data from *Lange and Carmichael* [1987], *Bottinga et al.* [1983], *Robie et al.* [1978], *Jeanloz and Thompson* [1983], and *Skinner* [1966].

alkalies), whose crystalline oxides are dense, often close-packed structures, are in similarly high-density local environments in silicate melts at 1 atm Given the similarity between the partial molar volumes of these oxides in melts and the volumes of densely packed crystalline oxides, we would expect that initially no great decreases in the partial molar volumes of these components in the melt will occur with increasing pressure, other than those also observed in the crystalline oxides due to simple compression.

The situation for the "network-forming" components (Al_2O_3, Fe_2O_3, and SiO_2) is different. The 1-atm partial molar volume of silica at 1400°C in liquids similar in composition to typical magmas is approximately equal to the volume of cristobalite, the stable polymorph of SiO_2 at 1400°C (Figure 7) Si is tetrahedrally coordinated by oxygen ions in cristobalite. The partial molar volume of silica in melts at 1 atm is, however, almost a factor of 2 higher than the molar volume of metastable stishovite under similar conditions. These observations are consistent with the essentially universally held conviction that Si is tetrahedrally coordinated by oxygen ions in silicate melts at low pressures The much higher values of the partial molar volumes of Al_2O_3 and Fe_2O_3 in silicate melts at 1 atm than the molar volumes of corundum and hematite similarly suggest that Al and Fe^{3+} are also dominantly tetrahedrally coordinated by oxygen in silicate melts at low pressure. Likewise, the high ratio of the partial molar volume of TiO_2 in Na-bearing, Ca-free melts relative to the volume of anatase suggests that Ti^{4+} is tetrahedrally coordinated by oxygen in such liquids.

It has been suggested that under conditions of sufficiently high pressures, Si and Al in melts convert nearly entirely to octahedral coordination from the tetrahedral coordination characteristic of low pressures [e.g., *Waff*, 1975; *Matsui and Kawamura*, 1980, 1984; *Matsui et al.*, 1982; *Angell et al.*, 1982, 1983, 1987; *Ohtani et al.*, 1985]. We suggest, based on the similarities between partial molar volumes of network-breaking components in silicate melts at 1 atm and the molar volumes of their crystalline oxides (Figure 7), that if Si, Al, and Fe^{3+} become octahedrally coordinated by oxygens in silicate melts, their partial molar volumes will be similar to within about 10% to the molar volumes of stishovite, corundum, and hematite. When full conversion to octahedral coordination has occurred, the volume of the melt would thus be expected to approach that of a mixture of dense oxides of the same composition, just as has been observed for multicomponent crystalline silicates at high pressures [e.g., *McQueen et al.*, 1967; *Al'tschuler and Sharipdzhanov*, 1971; *Svendsen and Ahrens*, 1983; *Boslough et al.*, 1986]

Using the equation of state parameters of Tables 4 and 8 and extrapolating the <25 GPa results of *Rigden et al.* [1988], we have calculated the volumes (per mole of oxygen atoms) of melts and of chemically equivalent mixtures of high pressure phases at 1400°C at both 1 atm and 40 GPa (Table 6) for the three compositions that we have studied on the anorthite-diopside join. Table 6 (column 6) shows that at 40 GPa, the volumes of these three melt compositions are, based on a best fit Birch-Murnaghan equation of state, within 10% of the equivalent mixtures of dense oxides. This is consistent with the hypothesis that Si and Al are nearly entirely octahedrally coordinated by oxygen in melts at this high pressure. The highest pressure shock wave data point for molten anorthite when corrected to a temperature of 1673 K yields a volume approximately equal to the calculated dense oxide mixture. The melt may really approach the solid volume this closely under these conditions, or as discussed by *Rigden et al.* [1988], crystallization could have occurred in this experiment, facilitated by a close approach in structure between liquid and solid at these very high pressures.

There is independent evidence for the approach of melt densities (and by inference, perhaps melt structures in the cases of melts with the compositions of individual minerals) to those of dense oxides at pressures of several hundred kilobars. *Lyzenga et al.* [1982] concluded, based on shock wave

TABLE 6. Volume/Oxygen of Molten Silicates and High-Pressure Phases at 1673 K

Composition	1 atm			40 GPa		
	$V_o^{m\,a}$	$V_o^{dp\,b}$	V_o^m/V_o^{dp}	$V_o^{m\,a}$	$V_o^{dp\,b}$	V_o^m/V_o^{dp}
$CaMgSi_2O_6$	13.73[c]	9.28	1.48	8.86[d]	8.02	1.10
$Di_{0.64}An_{0.36}$	13.63[c]	9.10	1.50	8.28[e]	7.89	1.05
$CaAl_2Si_2O_8$	13.51[c]	8.86	1.53	7.90[f]	7.71	1.03
	13.51[c]	8.86	1.53	7.67[d]	7.71	0.99

Units are $m^3\,mol^{-1} \times 10^{-6}$.
[a] Volume per mole of oxygens in the melt.
[b] Volume per mole of oxygens in a densely packed solid of the same composition, based on volumes of the dense crystalline oxides calculated from the data in Table 8.
[c] Calculated from *Stebbins et al.* [1984].
[d] Calculated using K_{0S}, K_S' from fit to full data set from this work.
[e] Calculated from <25 GPa equation of state data of *Rigden et al.* [1988].
[f] Calculated using K_{0S}, K_S' from five-point fit to molten anorthite shock data.

experiments in which they melted stishovite, that the molar volume of molten SiO_2 at 70 GPa is about 3% greater than that of crystalline stishovite. The experiments of *Jeanloz and Heinz* [1984], in which they determined the solidus of a magnesian silicate perovskite between 30 and 60 GPa, suggest that the liquid and solid volumes are very similar over this pressure range. Recently, *Brown et al.* [1987] analyzed shock temperature and Hugoniot data and presented new sound speed data along the Hugoniot of forsterite and $(Mg,Fe)_2SiO_4$ and concluded that, like stishovite, these compositions melt along the Hugoniot. The volume increase on melting at shock temperatures of $\sim$ 4000 K and pressures of 130 GPa appears to be $\lesssim$ 1%.

Although the suggestion that coordination changes involving Al and Si are important responses of silicate melt structures to increasing pressure is not new, there has been considerable uncertainty about whether coordination changes involving Al^{3+} in melts would occur abruptly over a narrow pressure range at about 1-2 GPa [*Waff*, 1975; *Kushiro*, 1980; *Boettcher et al.*, 1982, 1984] or more gradually over a wide interval centered at a somewhat higher pressure [e.g., *Angell et al.*, 1982, 1983, 1987; *Matsui and Kawamura*, 1984; *Ohtani et al.*, 1985]. It is generally accepted that Al will convert to greater than tetrahedral coordination in melts at lower pressures than Si, by analogy with crystalline solids and based on the results of computer simulations [*Matsui and Kawamura*, 1984; *Ohtani et al.*, 1985; *Angell et al.*, 1987].

Our results support the hypothesis that Al coordination changes are gradual, unless they are completed at pressures lower than the lowest that we have studied in our experiments. The smooth compression curves obtained for the compositions studied and the similarity in shape of the $\rho - P$ curves for our compositions, independent of Al content, suggest this. Shock wave studies of molten alkali halides at pressures up to $\sim$30 GPa (e.g., CsI) also show continuous compression curves and these too have been interpreted in terms of gradual increases in coordination numbers with pressure [*Ross and Rogers*, 1985]. Although we cannot rule out abrupt density changes in pressure intervals between our data points, conversion of all of the Al from tetrahedral to octahedral coordination would result in density jumps of $\sim$ 0.2 M g^{-3} and $\sim$ 0.1 M g^{-3} in the anorthite and anorthite-diopside compositions. These changes should be ultimately detectable via our experiments if they occur over narrow pressure intervals

The smooth compression curves that we have observed for the three compositions studied are also consistent with a gradual transformation of Si from tetrahedral to octahedral coordination over a pressure interval of several tens of gigapascals. Density increases of $\sim$0.6-0.9 M g^{-3} would be expected to accompany this structural change in the compositions studied; these would be difficult to miss in our data, even if they occurred over narrow pressure intervals between data points.

Compositional dependence of the elastic properties of silicate melts: The zero-pressure bulk modulus K_{0S}. Based on the present results and those of *Rigden et al.* [1988], the 1-atm bulk moduli of liquids in the system anorthite-diopside are only weakly dependent on composition, varying from 18 to 22 GPa for anorthite, to 24 GPa for the 1 atm eutectic composition, to 22 GPa for pure diopside Similar values (Table 7) were obtained by *Rivers* [1985] and *Rivers and Carmichael* [1987] by ultrasonic measurements and by *Bottinga* [1985] Molten fayalite at 1653 K has a similar bulk modulus of 21 4 GPa [*Rivers*, 1985]. This lack of variation in compressibility with composition is surprising. It is widely believed, based on analogy with their crystalline equivalents and on a variety of spectroscopic investigations [*Taylor and Brown*, 1979; *Sharma and Yoder*, 1979; *Sharma et al.*, 1983], that the structures of molten anorthite, diopside, and fayalite at 1 atm are very different. Anorthitic liquid is thought to be an essentially fully polymerized network of silicate and aluminate tetrahedra, probably with four-membered rather than six-membered rings [*Taylor and Brown*, 1979; *Sharma et al.*, 1983], (but see *Matsui and Kawamura*, [1984]); diopsidic melt is thought to be less polymerized, perhaps closely related to the crystalline diopside structure with well-defined, perhaps close-packed arrangements of network-breaking components at the boundaries of silicate polymers or clusters [e.g., *Sharma and Yoder*, 1979; *Greaves et al.*, 1981; *Gaskell*, 1982; *Greaves*, 1983]; and fayalitic melt, like crystalline olivine, would generally be supposed to be based on something approaching

TABLE 7. Values of K_{OS} Based on Shock Wave and Ultrasonic Data

Composition	Temperature K	Birch-Murnaghan Equation, GPa	Shock-Particle Velocity Relation, GPa	Ultrasonic,[a] GPa
Diopside (Di)Ca Mg Si_2O_6	1773	22.4[b]	28.4	24.2
$Di_{0.64}$ $An_{0.36}$	1673	24.2[b]	24.4	22.3
Anorthite (An)$CaAl_2Si_3O_8$	1923	17.9[b,d], 22.0[c]	18.3[b,d], 20.9[c]	20.6

[a] *Rivers* [1985]; *Rivers and Carmichael* [1987].
[b] Preferred value.
[c] Six-point fit.
[d] Five-point fit.

close packing of oxygen atoms in which silicate tetrahedra are largely unlinked. We therefore expected that at 1 atm, molten anorthite would be significantly more compressible than molten diopside (since its tetrahedral framework would be more capable of distortions via bending of the T-O-T (tetrahedral-oxygen-tetrahedral) angles and since the more open tetrahedral framework would be expected to be more compressible than the more compact diopsidic structure; this line of reasoning correctly anticipates the very low bulk 1-atm modulus of silica glass) which in turn would be more compressible than molten fayalite. Clearly, the notion that degree of polymerization of aluminosilicate tetrahedra correlates in some simple way with compressibility is incorrect for certain molten silicates at 1 atm

At least part of the explanation for the similarity in the bulk modulus of molten anorthite, diopside, and olivine may be that melts of these compositions are very similar in the efficiency of their atomic "packing" at 1 atm. The volume per mole of oxygen atoms is essentially identical at 1673 K in molten anorthite, diopside and fayalite· 13.5-13.7 $m^3\ mol^{-1} \times 10^{-6}$. Surprisingly, the oxygen atoms in molten anorthite are actually more closely packed than in the pyroxene liquid

This observation, when coupled with the similarity in 1-atm bulk moduli of these liquids, leads us to suggest the following hypothesis: Molten anorthite, diopside, and olivine at 1 atm may be viewed as consisting of essentially similar packings of oxygen atoms with cations in the interstices It is interesting that the partial molar volume per oxygen atom for a variety of "network-forming" and "network-breaking" oxides (SiO_2, Al_2O_3, FeO, MgO, Fe_2O_3, TiO_2) in geologically relevant compositions falls into a narrow range (12-15 cm^3/mol at 1600°C [*Stebbins et al.*, 1984]); this is precisely the behavior to be expected if oxygen packing varied little with melt composition (If oxygen packing were independent of cationic chemistry, the partial molar volume per oxygen atom would be identical for all oxides.) An increase in pressure results in a gradual collapse of this packing arrangement. The precise nature of this collapse is unknown, though presumably it leads ultimately, as discussed in the preceding section, to higher geometric coordination of Si, Al, and Fe^{3+} by oxygen ions One possibility is that suggested by *Stolper and Ahrens* [1987]. They suggest that decreasing intertetrahedral angles can lead to a continuous rearrangement from tetrahedral to octahedral coordination of cations such as Si^{+4} by oxygen ions It could also involve reductions in the number of defects in the structure or changes in the ring structures of Si^{+4} tetrahedra.

We do not want to give the incorrect impression that 1-atm bulk moduli or volumes per oxygen melts are all the same. For example, based on the data summarized by *Stebbins et al.* [1984], the volume per oxygen atom of molten forsterite is about 8% lower than that for molten fayalite. However, the 1-atm bulk modulus expected for metastable forsteritic liquid at 1400°C is about 25 GPa [*Rivers*, 1985]; again, this is not too different from the values that we have discussed above. In addition, larger cations, particularly the alkalies and the large alkaline earths, have higher partial molar volumes per oxygen, and their presence in melts leads to significantly lower 1-atm bulk moduli [*Rivers and Carmichael*, 1987]. The change in the partial molar volume per oxygen with pressure at 1 atm is roughly independent of the size of the cation below a certain partial molar volume per oxygen ($\sim 30\ m^3\ mol^{-1} \times 10^{-6}$); above this critical value of partial molar volume, the change in the partial molar volume per oxygen with pressure increases regularly with cation size (Figure 8). In the context of our proposed rationalization of the near constancy of K_{OS} and volume per oxygen atom over a wide range of melt compositions, we would explain the effects of these large cations as follows: When the smaller cations are present, although they influence the pressure derivative of volume (i.e., K_{OS}), oxygen-packing considerations and oxygen-oxygen interactions dominate the compression of the melt However, the larger alkali cations do not readily fit into the holes between the oxygen atoms in roughly close packing, so that the oxygens must be sprung apart to accommodate them. Cation-oxygen bonds, which have a large compliance for the large alkali atoms will dominate the compression in these situations, and thus compressibility increases dramatically as these alkalies are added to the melt.

Compositional dependence of the elastic properties of silicate melts: The pressure derivative of bulk modulus K' Although the 1-atm volumes per oxygen atom and bulk moduli of melts along the join anorthite-diopside and molten fayalite are similar, the pressure derivative of the bulk modulus K' shows substantial variations with composition. It varies from 4 to 5 for anorthite melt to 7 for diopside melt based on our data, to 10-14 for molten fayalite based on *Rivers'* [1985] analysis of the position of the solidus. In this section, we attempt a simple rationalization for the substantial variations observed in K'

We must first emphasize, however, that the use of Birch-Murnaghan equation of state to describe the behavior of complex silicate liquids over a pressure range of several hundred kilobars must be, at best, an oversimplification It is well known that the compression of silica glass cannot be

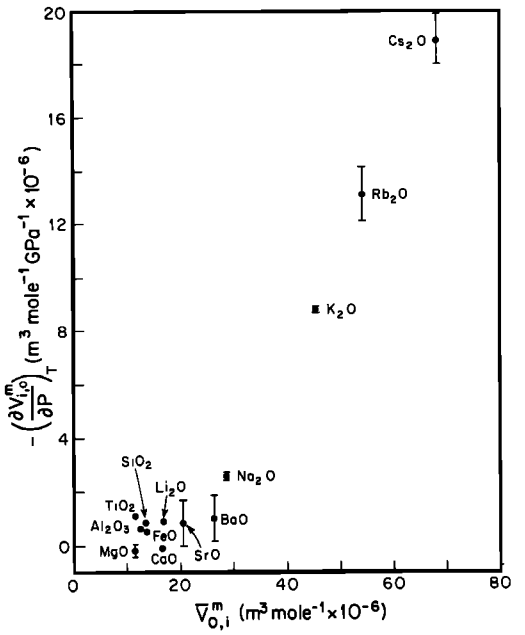

Fig. 8. Variation of change in partial molar volume per oxygen with pressure $\left((\partial V_{o,i}^m)/(\partial P)\right)_T$ [*Rivers and Carmichael,* 1987; *Lange and Carmichael,* 1987] for silicate melts with partial molar volume per oxygen of oxide components ($\bar{V}^m_{o,i}$). Below $\bar{V}^m_{o,i} \sim 30$ m^3 mol^{-1} $\times$ 10^{-6}, $\left((\partial V_{o,i}^m)/(\partial P)\right)$ is essentially independent of $\bar{V}^m_{o,i}$. Data from same sources as Figure 7.

described adequately by a single, simple equation of state [*Bridgman and Simon,* 1953; *Peselnick et al.,* 1967, *Schroeder et al.,* 1981; *Meade and Jeanloz,* 1987]. Similarly, there is no reason, a priori, to expect that density changes reflecting conversion of Al^{3+} and Si^{4+} to octahedral coordination with increasing pressure can be described by a simple Birch-Murnaghan equation. In addition, if the coordinations of different cations respond differently to pressure, a single Birch-Murnaghan equation would probably be inadequate. It is important to recognize that the K_{0S} and K' values that we have derived from our data are averaged over the entire pressure interval that we have studied experimentally and are dependent on the choice of the Birch-Murnaghan equation of state.

Nevertheless, the values of K_{0S} derived from our data are very similar to those determined independently by ultrasonic measurements [*Rivers,* 1985] and successfully recover the solidus of diopside up to 50 kbar (Figure 5). Unless this agreement is fortuitous, the simplest explanation of these facts is that the compression mechanisms at low pressure probed by the ultrasonic measurements and the phase equilibria are continuous with those probed at higher pressure by our shock wave studies [*Rigden et al.,* 1988]. Though surprising and probably not true in every detail, we feel that this statement, with its implication that changes leading to increased coordination of Al and Si by oxygen begin at very low pressures, is the likely explanation for the similarity in the various estimates of K_{0S}. As discussed by *Rigden et al.* [1988] and *Stolper and Ahrens* [1987], it is possible to envision mechanisms for achieving higher coordinations of Al and Si by distortions in a tetrahedral network that could well be continuous from 1 atm up to tens of gigapascals.

Suppose that two melts (e.g., molten anorthite and diopside) differ in chemistry but have essentially identical bulk moduli at 1 atm. Presuming that most of the difference in compression between the two melts over a pressure range of several hundred kilobars will reflect differences in the concentrations of cations that will convert from tetrahedral to octahedral coordination, the more aluminous and silica-rich composition would experience more compression over this pressure interval, and hence its bulk modulus averaged over this pressure interval would be lower. As a result, the rate of increase in K with pressure for the more Al-Si-rich melt will be lower over the pressure interval in which these coordination changes occur, and its value of K' averaged over this pressure interval will be lower We would thus expect, as is indeed observed, that K' increases for melts in the order anorthite $\rightarrow An_{0.36}Di_{0.64}\rightarrow$ diopside. We can, in addition, predict that Al- and Si-poor melts such as fayalite will not experience as much compression as feldspar- and pyroxene-rich compositions, and thus that they will have relatively high values for K', given that they have 1-atm bulk moduli similar to feldspathic and pyroxenitic melts Using this concept and the 1-atm bulk moduli from systematic ultrasonic studies [*Rivers,* 1985], it is possible to estimate values of K' for different melt compositions.

We first note that the Hugoniots of molten An, Di, and $Di_{0.64}An_{0.36}$ approach those of the equivalent solid materials at ~40 GPa (Table 6 and Figures 3 and 4; also, Figure 9 of *Rigden et al.* [1988]). We also observe that the Hugoniots of the silicates in the high-pressure regime are well approxi-

TABLE 8. STP, Equations of State Parameters of Oxides, Used to Construct High-Temperature Equation of State

Oxide	Density, Mg/m^3	Isentropic Bulk Modulus K_{0S}, GPa	$(\partial K_s/\partial P)_s$	Grüneisen Parameter
Al_2O_3	3.988	252.7[a]	4.3[a]	1.32[a]
CaO	3.345	112.0[b]	4.8[b]	1.51[b]
FeO	5.864	158[c]	4[c]	1.63[b]
MgO	3.584	162.7[a]	4.27[a]	1.32[a]
SiO_2	4.290	316.0[d]	4[e]	1.25[e]

[a] *Anderson et al.* [1968].
[b] *Jeanloz and Ahrens* [1980].
[c] *Jeanloz and Sato-Sorensen* [1986].
[d] *Weidner et al.* [1982].
[e] *Lyzenga et al.* [1982].

TABLE 9. Equation of State Parameters for Molten Silicate at 1673 K

Silicate	1 atm Molar Volume (1673 K)[a] μm^3/mol oxygen ion	Isothermal Bulk (1673 K) GPa	$(\partial K_T/\partial P)_T$[c]
Fe_2SiO_4	13.53	20.5	11.2
Mg_2SiO_4	12.67	24.9	10.2
$MgSiO_3$	12.90	21.8	6.8
$FeSiO_3$	13.47	17.6	8.0
$CaMgSi_2O_6$	13.73	23.8	7.1
$An_{0.36}Di_{0.64}$	13.63	22.3	7.0
$CaAl_2Si_2O_8$	13.51	20.5	6.9

[a] *Stebbins et al.* [1984].
[b] Calculated from *Rivers* [1985] and *Rivers and Carmichael* [1987].
[c] Present study. Uncertainties can be as large as ± 1.5

mated by a mixture of dense-packed oxides [e.g. *McQueen et al.*, 1967; *Al'tschuler and Sharipdzhanov*, 1971, *Svendsen and Ahrens*, 1983; *Boslough et al.*, 1986] We assume that upon compression of melts to 40 GPa, Si^{+4} and Al^{+3} ions transform from fourfold to at least sixfold coordination with oxygen. The melt at 40 GPa is assumed to be 10% less dense than equivalent oxide mixture, whose density is calculated using equation of state data for dense oxides (Table 8) We then determine the value of K′ that given the 1-atm compressibility of the melt from ultrasonic studies [*Rivers*, 1985; *Rivers and Carmichael*, 1987] and the 1-atm density [*Stebbins et al.*, 1984], gives this value for the 40 GPa density. In addition to the parameters given in Table 8, we assume that γ/V is a constant for the oxides and the specific heat at constant volume is 3R per mole of atoms

The equation of state for a range of molten silicates, at 1673 K, based on this calculation, including the predicted value of $(dK_T/\partial P)_T$, is given in Table 9 As is demonstrated in Figure 9, the predicted values of $(dK_T/\partial P)_T$ define some systematic relationships The estimates of K_T' for enstatite (6.8) and ferrosilite (8 0) melts are similar to the experimentally determined value for molten diopside (6.9); as expected, the values of K_T' for molten forsterite (10.2) and fayalite (11.2) are higher than those we have found for pyroxene and plagioclase in our experiments. The estimate for molten anorthite (6.9) is similar to, but somewhat higher than, our measured value (4 1-5 3). The sensitivity of the above values of K_T' are as follows· If the pressure at which $V_{melt}/V_{oxide} = 1\ 10$ is varied by 5 GPa, the values of K_T' vary by ± 0 3 If the criteria are changed to $V_{melt}/V_{oxide} = 1\ 05$, which is also consistent with the last column of Table 6, the estimated values of K_T' are decreased by ~ 1.5

We have generalized our limited data a long way in suggesting that all melts will bear the same relation (approximately 10% less dense) to dense high-pressure phases at 40 GPa, and even according to our results this is only approximately correct. Nevertheless, this simple approach does agree well with the high values of K_T' (10-14) implied for fayalite melt by the completely independent fit to the solidus [*Rivers*, 1985]. It also suggests a simple rule of thumb that, if substantiated by further experiments, would be extremely valuable in thinking about the densities of melts at high pressures. The volumes per oxygen at 40 GPa of stishovite and corundum are significantly lower than the other common oxides (e.g., at 1673 K, these volumes are about 6.5 and 7.8 $m^3\ mol^{-1} \times 10^{-6}$, respectively, compared with values of 9.5-13 $m^3\ mol^{-1} \times 10^{-6}$ for MgO, CaO, and FeO and 28-43 $m^3\ mol^{-1} \times 10^{-6}$ for Na_2O and K_2O). Therefore the ultimate high-pressure volumes of melts rich in silica and alumina will be lower than those of melts poor in these constituents. Given that 1-atm volumes and bulk moduli of common silicate compositions are similar, this suggests that silica- and alumina-rich melts will have low values of K′ relative to more basic melts.

CONCLUSIONS

1. Shock wave equation of state measurements on molten diopside and anorthite complement the existing data on an intermediate composition and enable inferences to be made about the effect of composition on compressibility. For molten diopside we calculate a value of $K_{0S} = 22.4$ GPa and $K_S' = 6.9$ at 1773 K compared with the ultrasonically determined value of $K_{0S} = 24\ 2$ GPa at 1758 K [*Rivers*, 1985]. Two different fits to the results for molten anorthite at 1923 K were calculated. For the entire data set, $K_{0S} = 22\ 0$ GPa and $K_S' = 4.1$ When the highest pressure point was omitted from the fit, the rms was reduced slightly, giving $K_{0S} = 17.9$ GPa, $K_S' = 5.3$. *Rivers* [1985] gives $K_{0S} = 20.6$ GPa at 1833 K based on ultrasonic measurements

2. Using the new equation of state of molten diopside (and existing data for solid diopside), we place constraints on the slope (dT/dP) of the fusion curve at high pressures. We expect that the slope will be shallow at pressures above 10 GPa, but in the absence of constraining data on the variation in the Gruneisen parameters for crystal and liquid or the changes of α_P for these phases with pressure, a precise determination of the high-pressure fusion curve is difficult. Our best fits to the experimental solidus data (<5 GPa) use a model for γ/V equal to a constant or a model in which $\Delta(\alpha_P V)$ decreases linearly with pressure until it reaches zero.

3 The volume of the intermediate $An_{0.36}Di_{0.64}$ melt composition can be calculated to within 1.5% based on ideal mixing of the molten anorthite and diopside end-members at pressures up to 25 GPa despite the fact that volumes decrease about 30% over this pressure range If approximately ideal mixing for volumes can be shown to hold over a range of compositions, it will be useful in calculations of the melts densities at elevated pressures

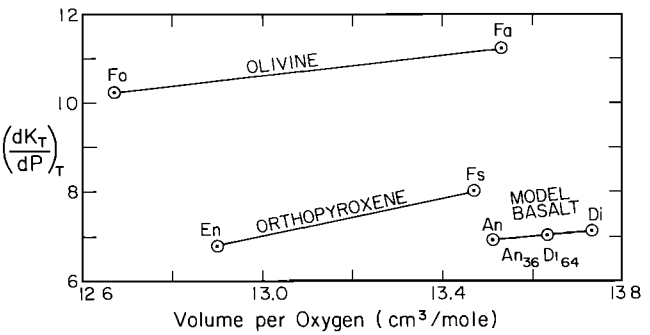

Fig. 9. Predicted values of $(\partial K_T/\partial P)_T$ at 1673 K for molten silicates versus volume per mole oxygen ions.

4. Our results support the hypothesis that the coordinations of Al^{3+} and Si^{4+} by oxygen change from tetrahedral at low pressures to octahedral at high pressures and that by 30-40 GPa, nearly all of these cations are octahedrally coordinated. Our data also suggest that these changes occur continuously and gradually over several tens of gigapascals beginning at 1 atm If such coordination changes occurred over narrow pressure intervals, they would be detectable in our Hugoniot density measurements. This would be particularly dramatic for Si

5. Bulk moduli at 1 atm for molten silicates are similar for a wide range of compositions of petrological interest, based on both our experimental data and from ultrasonic measurements of *Rivers* [1985], but the pressure derivative of bulk modulus varies significantly with composition We suggest that this results from similar packing of oxygen atoms in silicate liquids over this composition range at atmospheric pressure and that the degree of compression at higher pressures is primarily related to the ability of the structure to collapse by coordination changes of Al^{3+}, Si^{4+}, and Fe^{3+} from tetrahedral to octahedral. For similar values of 1 atm bulk modulus this would be reflected in higher values of K_T' for Al^{3+}, Si^{4+}, Fe^{3+}-poor melts. At $\sim$ 40 GPa, melts are proposed to achieve $\sim$ 1 0-1.1 times the volume of dense high-pressure crystalline phases at this pressure

6. Estimates of K_T' for molten silicates, assuming that their volumes are 10% greater than mixtures of crystalline dense phases at 40 GPa, have been made using 1-atm bulk moduli calculated from *Rivers* [1985] and *Rivers and Carmichael* [1987] The olivine liquids, molten fayalite and forsterite, have K_T' $\sim$ 9-11, and pyroxene liquids, molten enstatite and ferrosilite, have K_T' $\sim$ 7 - 8, similar to molten diopside. These values of K_T' can be uncertain by $\pm$1 5. Our estimate of K_T' for fayalite is consistent with the value calculated by *Rivers* [1985] from an analysis of its fusion curve up to its 7-GPa triple point.

Appendix Fusion Curve for Diopside

To calculate the fusion curve of diopside (assuming congruent melting), we use the Clausius-Clapeyron relation in two different forms. One simple form, in which we assume a constant specific heat for both liquid and solid at 3R per mole, and γ/V (Table 5) as a constant leads to

$$\frac{dTm}{dP} = \frac{\Delta V_{fusion}}{\Delta S_{fusion}} = \frac{V_L(P,Tm) - V_C(P,Tm)}{\Delta S_f^o + 3R\left[ln(T_{M,P}/T_S^L) - ln(T_{M,P}/T_S^C)\right]} \quad (1)$$

where $V_L(P,Tm)$ and $V_C(P,Tm)$ are the molar volumes of the liquid and crystal at the pressure P and melting point Tm. Here ΔS_f^o is the entropy of fusion at 1 atm and T_o For the present calculation we take T_o = 1664 K, and R has the usual meaning. Here T_S^L and T_S^C are the temperature along the isentropes of the liquid and solid, respectively, centered at 1 atm and T_o at the same specific volumes as the liquid and solid at the pressure of the melting point. Thus the two logarithm terms give the increase in entropy upon heating (at constant volume) from the temperature of the isentrope (at volumes of the melting point) to the melting point. The fusion curve obtained from integrating equation (1) is labeled γ/V = constant in Figure 5. Only by strongly varying drastically from the Table 5 values to γ_o = 2.4 and 0.01 for the crystal and liquid, respectively, is the dashed curve of Figure 5 obtained which is required to fit the fusion curve of *Scarfe and Takahashi* [1986].

A second rather different calculation may be carried out using

$$\frac{dT_M}{dP} = \frac{\Delta V_{fusion}}{\Delta S_{fusion}} = \frac{\Delta V_f^o + \int_{0,T_0}^{P,T_0} \Delta\left[\frac{\partial V}{\partial P}\right]_T dP + \int_{T_{0,P}}^{T_{M,P}} \Delta\left[\frac{\partial V}{\partial T}\right]_P dT}{\Delta S_f^o + \int_{T_{0,0}}^{T_{M,0}} \Delta\left[\frac{\partial S}{\partial T}\right]_P dT + \int_{0,T_M}^{P,T_M} \Delta\left[\frac{\partial S}{\partial P}\right]_T dP} \quad (2)$$

where ΔV_f^o is the volume change of fusion at 1 atm and T_0 (1665 K), and the integrands $\Delta(\partial V/\partial P)_T$, $\Delta(\partial V/\partial T)_P$, $\Delta(\partial S/\partial T)_P$, and $\Delta(\partial S/\partial P)_T$ represent the additional terms required to describe the change in volume and entropy upon fusion at high temperature and pressure In estimating these terms we employ the thermodynamic relations

$$\left[\frac{\partial V}{\partial P}\right]_T = -\beta_T V \quad (3)$$

$$\left[\frac{\partial S}{\partial P}\right]_T = -\left[\frac{\partial V}{\partial T}\right]_P = -\alpha_P V \quad (4)$$

$$\left[\frac{\partial S}{\partial T}\right]_P = \frac{C_P}{T} \quad (5)$$

where α_P is the isobaric coefficient of thermal expansion, β_T is the isothermal compressibility, and C_P is the isobaric heat capacity (Table 5). Recent compilations of heat capacity, entropy of fusion, and volume of molten silicates have been made by two separate groups [*Richet and Bottinga*, 1984; *Bottinga et al.*, 1982, 1983; *Stebbins et al.*, 1984] These results were used in conjunction with our equation of state for molten diopside to estimate the position of the solidus of diopside

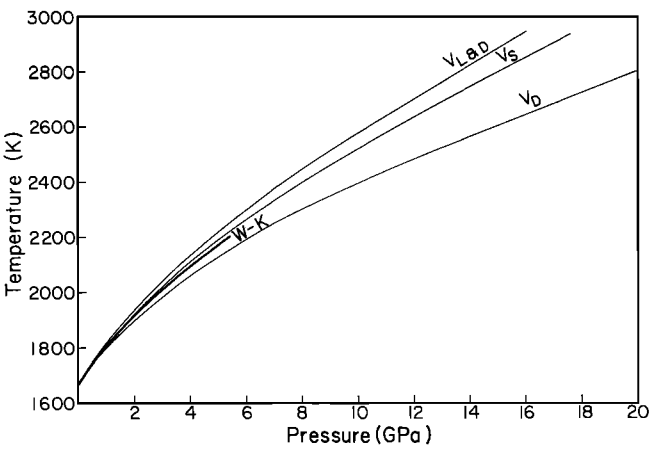

Fig. A1a. Effect of different initial liquid volumes on predicted fusion curve of diopside. ($V_{L\&D}$, *Licko and Danek* [1982]; V_S, *Stebbins et al.* [1984]; V_D, *Dane* [1941]).

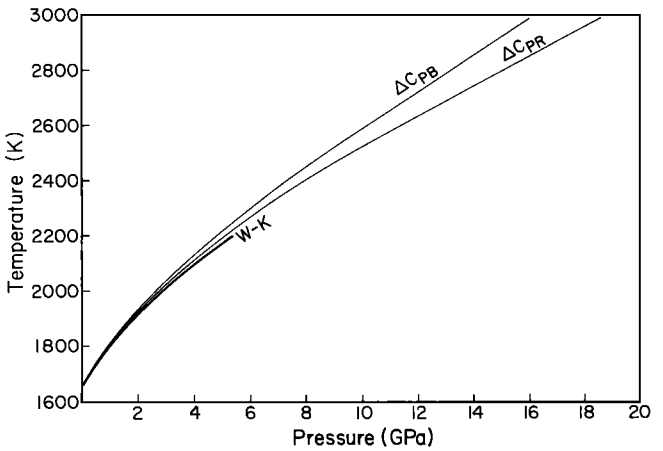

Fig. A1b. Effect of different heat capacity functions on predicted fusion curve of diopside (ΔC_{PB}, *Bottinga* [1985]; ΔC_{PR}, *Rivers* [1985]).

Although a large and growing data base on the thermodynamic properties of molten and crystalline silicates, including diopside, has become available in recent years, the uncertainties in their values, particularly as functions of temperature and pressure, translate into substantial uncertainties in the calculated position of the diopside solidus This is demonstrated in Figures A1a-A1c in which we compare several calculations of the diopside solidus with experimental determinations to 5 GPa. All of the calculated curves emanate from the same 1-atm "melting point," taken as the solidus of diopside, 1664 K [*Kushiro*, 1972], and all employ the same equation of state for the melt

In Figure A1a the input parameters that result in a range of calculated solidi differ only in the choice of the 1-atm volume of diopside liquid. *Rivers* [1985] pointed out that the small differences between the measured values of *Dane* [1941] and *Licko and Danek* [1982] and the calculated values from the compilations of *Bottinga et al.* [1983] and *Stebbins et al.* [1984] translate into differences in the calculated fusion curves at pressures greater than 5 GPa The liquid

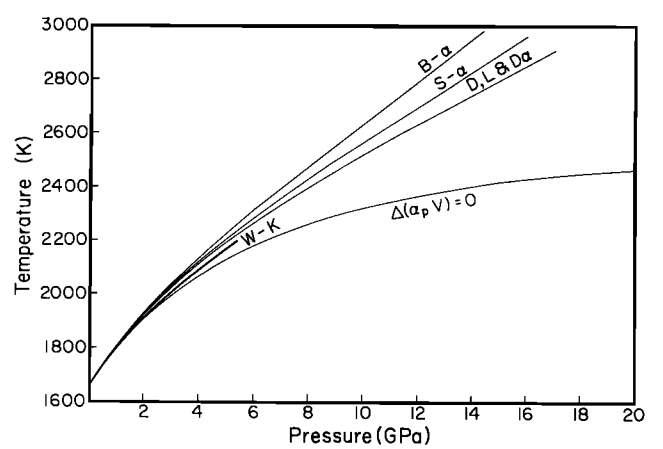

Fig. A1c. Effect of changing the thermal expansion of molten diopside on predicted fusion curve of diopside (for $\Delta(\alpha_p V)$ equal to 1 atm value; B-α, *Bottinga et al.* [1983]; S-α, *Stebbins et al.*, [1984]; (D,L&D-α, *Dane* [1941]; and *Licko and Danek* [1982]). Curve labelled $\Delta(\alpha_p V) = 0$ is calculated assuming that the thermal expansions of molten and crystalline diopside are the same.

at the solidus at 1 atm differs slightly in composition from pure diopside The unknown degree to which this incongruent melting behavior persists at high pressures also contributes to the uncertainties in the uncompressed liquid volume

In Figure A1b, we demonstrate the effect of varying values of C_P of the liquid phase The 1-atm values of *Stebbins et al.* [1984] and *Bottinga* [1985], although slightly different, have the effect indicated in Figure A1c when the fusion curve is extrapolated

An equally important uncertainty in these calculations arises from the unknown effect of pressure on α_P for the liquid and solid. In particular, we must know the variation of $\Delta(\alpha_P V)$ with pressure in order to carry out this calculation as this parameter enters into both the numerator and denominator of (2) through (4) This parameter varies with pressure according to

$$\frac{\delta}{\delta P}(\alpha_P V) = \alpha_P \frac{\delta V}{\delta P} + V \frac{\delta \alpha}{\delta P} \tag{6}$$

From the 1-atm compressibilities we can obtain $\delta V/\delta P$, and using the relation $\delta\alpha/\delta P = -\delta\beta/\delta T$, we can obtain $\delta\alpha/\delta P$. For both molten and crystalline diopside $\delta(\alpha_P V)/\delta P$ is small compared with $\alpha_P V$, but the initial slope calculated at 1 atm and 1673 K is about 3 times as great for the liquid as for the crystal, suggesting that $\Delta(\alpha_P V)$ decreases with increasing pressure. Maximum and minimum estimates of the slope of the solidus at any pressure can be made by assuming that $\Delta(\alpha_P V)$ is either equal to its 1-atm value or to zero These two extremes are compared in Figure A1c for several different estimates of $\Delta(\alpha_P V)$.

It is expected that the actual value of $\Delta(\alpha_P V)$ lies between the two extremes of Figure A1c. The first assumption ($\Delta(\alpha_P V)$ = 1 atm value) will be more valid at low pressures, whereas the second ($\Delta(\alpha_P V) = 0$) would be more valid at high pressures. Using the relation for $\delta(\alpha_P V)/\delta P$ of equation (6), we have calculated this value for both molten and solid diopside at 1 atm, reducing $\Delta(\alpha_P V)$ as a function of pressure until $\Delta(\alpha_P V) = 0$. For the calculated values of $\delta(\alpha_P V)/\delta P$ this occurs at $\sim$ 9 GPa. At higher pressures we assume $\Delta\alpha_P V = 0$ The fusion curve obtained in this way is labeled as $\Delta(\alpha_p V)=0$ in Figure 5 This calculation gives a lower solidus curve than the 5 GPa corrected curve (W-K_c) of *Williams and Kennedy* [1969] but is $\sim$50°C above the curve of *Irifune and Ohtani* [1986] at 10 GPa.

Acknowledgments. We wish to thank E. Bus, E. Gelle, C. Manning, M. Long, and L. Young for their invaluable technical help. R. Heuser carried out microprobe analyses. We have benefited from discussions with C.A. Angell, J. Bass, P.H. Gaskell, R. Jeanloz, and B. Kamb. We appreciate the use of the 10 kW R-F heater provided by L.T. Silver. Support was provided by NSG grant EAR84-07784. Division of Geological and Planetary Science, California Institute of Technology, Pasadena, California, contribution 4370.

REFERENCES

Agee, C. B., and D. Walker, Static compression and olivine flotation in ultrabasic silicate liquids, *J. Geophys. Res.*, *93*, 3437-3449, 1988.

Ahrens, T.J., J.T. Rosenberg, and M.H. Rudeman, Dynamic properties of rocks, *Final Rep., DA-45-146-X2-277*, SRI Proj. FGU-4816, Stanford Res. Inst., Menlo Park, Calif., 1966.

Al'tschuler, L.V., and I.I. Sharipdzhanov, Additive equations of state of silicates at high pressures, *Izv. Acad. Sci. USSR Phys. Solid Phys.*, Engl. Transl., *9*, 11-28, 1971.

Anderson, O.L., E. Schreiber, R.C. Leibermann, and N. Soga, Some elastic constant data on minerals relevant to geophysics, *Rev. Geophys., 6,* 491-524, 1968.

Angell, C.A., P.A. Cheeseman, and S. Tamaddon, Pressure enhancement of ion mobilities in liquid silicates from computer simulation studies to 800 kilobars, *Science, 218,* 885-887, 1982.

Angell, C.A., P.A. Cheeseman, and S. Tamaddon, Water-like transport property anomalies in liquid silicates investigated at high T and P by computer simulation techniques, *Bull. Mineral., 106,* 87-97, 1983.

Angell, C.A., P.A. Cheeseman, and R.R. Kadiyala, Diffusivity and thermodynamic properties of diopside and jadeite melts by computer simulation studies, *Chem. Geol., 62,* 83-92, 1987.

Biggar, G.M., and M.J. O'Hara, Solid solutions at atmospheric pressure in the system CaO-MgO-SiO_2 with special reference to the instabilities of diopside, akermanite, and monticellite, *Prog. Exp. Pet. 1st Rep.,* pp. 86-96, NERC, London, 1969.

Boettcher, A.L., C. Wayne Burnham, K.E. Windom, and S.R Bohlen, Liquids, glasses and the melting of silicates to high pressures, *J. Geol., 90,* 127-138, 1982.

Boettcher, A., Q. Guo, S. Bohlen, and B. Hanson, Melting in feldspar-bearing systems to high pressures and the structure of aluminosilicate liquids, *Geology, 12,* 202-204, 1984.

Boslough, M.B., S.M. Rigden, and T.J. Ahrens, Hugoniot equations of state of anorthite glass and lunar anorthosite, *Geophys. J. R. Astron. Soc., 84,* 455-473, 1986.

Bottinga, Y., On the isothermal compressibility of silicate liquids at high pressure, *Earth Planet. Sci. Lett., 74,* 350-360, 1985.

Bottinga, Y., and D.F. Weill, Densities of silicate liquid systems calculated from partial molar volumes of oxide components, *Am. J. Sci., 269,* 169-182, 1970.

Bottinga, Y., D. Weill, and P. Richet, Density calculations for silicate liquids, I, Revised method for aluminosilicate compositions, *Geochim. Cosmochim. Acta, 46,* 909-919, 1982.

Bottinga, Y., P. Richet, and D.F. Weill, Calculation of the density and thermal expansion coefficient of silicate liquids, *Bull. Mineral., 106,* 129-138, 1983.

Boyd, F.R., and J.L. England, Effect of pressure on the melting of diopside, $CaMgSi_2O_6$, and albite, $NaAlSi_3O_8$, in the range up to 50 kilobars, *J. Geophys. Res., 68,* 311-323, 1963.

Bridgman, P.W., and I. Simon, Effect of very high pressure on glass, *J. Appl. Phys., 25,* 405-413, 1953.

Brown, J.M., M.D. Furnish, and R.G. McQueen, Thermodynamics for $(Mg,Fe)_2SiO_4$ from the Hugoniot, in *High Pressure Research in Geophysics* edited by M.H. Manghnani and Y. Syona, Terra Scient. Publish. Co., Tokyo, pp. 373-384, 1987.

Dane, E.B., Jr., Densities of molten rocks and minerals, *Am. J. Sci., 239,* 809-818, 1941.

Finger, L.W., and Y. Ohashi, The thermal expansion of diopside to 800°C and a refinement of the crystal structure at 700°C, *Am. Mineral., 61,* 303-310, 1976.

Gaskell, P.H., A structural interpretation of the density of alkali silicate glasses, *J. Phys., 43,* C9:101-C9:105, 1982.

Goldsmith, J.R., The melting and breakdown relationships of anorthite at high pressures and temperatures, *Am. Mineral., 65,* 272-283, 1980.

Greaves, G.N., Glass: A look inside, *New Sci., 97,* 246-248, 1983.

Greaves, G. N., A. Fontaine, P. Lagarde, D. Raoux, and S. J. Gurman, Local structure of silicate glasses, *Nature, 293,* 611-616, 1981.

Herzberg, C.T., Solidus and liquidus temperatures and mineralogies for anhydrous garnet-lherzolite to 15 GPa, *Phys. Earth Planet. Inter., 32,* 193-202, 1983.

Herzberg, C.T., Chemical stratification in the silicate Earth, *Earth Planet. Sci. Lett., 67,* 249-260, 1984.

Herzberg, C.T., Magma density at high pressure, Part I, The effect of composition on the elastic properties of silicate liquids in *Magmatic Processes: Physiochemical Principles,* edited by B.O. Mysen, pp. 25-46, *Geochemical Soc.,* Sp. Publ. 1, 1987a.

Herzberg, C.T., Magma density at high pressure, Part II, A test of the olivine flotation hypothesis, in *Magmatic Processes: Phyiochemical Principles,* edited by B.O. Mysen, pp. 47-58, *Geochemical Soc.,* Sp. Publ. 1, 1987b.

Irifune, T., and E. Ohtani, Melting of pyrope $Mg_3Al_2Si_3O_{12}$ up to 10 GPa: Possibility of a pressure-induced structural change in pyrope melt, *J. Geophys. Res., 91,* 9357-9366, 1986.

Jeanloz, R., and T.J. Ahrens, Equations of state of FeO and CaO, *Geophys. J. R. Astron. Soc., 62,* 505-528, 1980.

Jeanloz, R., and D. Heinz, Experiments at high temperature and pressure: Laser heating through the diamond cell, *J. Phys., 45,* C8:83-C8:92, 1984.

Jeanloz, R., and Y. Sato-Sorensen, Hydrostatic compression of $Fe_{1-x}O$ wüstite, *J. Geophys. Res., 91,* 4665-4672, 1986.

Jeanloz, R., and A.B. Thompson, Phase transitions and mantle discontinuities, *Rev. Geophys., 21,* 51-74, 1983.

Kushiro, I., Determination of liquidus relations in synthetic silicate systems with electron probe analyses: The system forsterite-diopside-silica at 1 atm, *Am. Mineral., 57,* 1260-1271, 1972.

Kushiro, I., Viscosity, density, and structures of silicate melts at high pressures, and their petrological applications, in *Physics of Magmatic Processes,* edited by R.B. Hargraves, pp. 93-120, Princeton University Press, Princeton, N.J., 1980.

Lange, R. A., and I. S. E. Carmichael, Densities of Na_2O-K_2O-CaO-MgO-FeO-Fe_2O_3-Al_2O_3-TiO_2-SiO_2 liquids, *Geochim. Cosmochim. Acta, 51,* 2931-2946, 1987.

Levien, L., and C.T. Prewitt, High-pressure study of diopside, *Am. Mineral., 66,* 315-323, 1981.

Licko, T., and V. Danek, Densities of melts in the system $CaSiO_3$–$CaMgSi_2O_6$–$Ca_2MgSi_2O_7$, *Phys. Chem. Glasses, 28,* 67-71, 1982.

Liu, L.-G., The system enstatite-wollastonite at high pressures and temperatures with emphasis on diopside, *Phys. Earth Planet. Inter., 19,* P15-P18, 1979.

Lyzenga, G.A., T.J. Ahrens, and A.C. Mitchell, Shock temperatures of SiO_2 and their geophysical implications, *J. Geophys. Res., 88,* 2431-2444, 1982.

Matsui, Y., and K. Kawamura, Instantaneous structure of an $MgSiO_3$ melt simulated by molecular dynamics, *Nature, 285,* 648-649, 1980.

Matsui, Y., and K. Kawamura, Computer simulation of structures of silicate melts and glasses, in *Materials Science of the Earth's Interior,* edited by I. Sunagawa, pp. 3-23, Terra Scientific, Tokyo, 1984.

Matsui, Y., K. Kawamura, and Y. Syono, Molecular dynamics calculations applied to silicate systems: Molten and vitreous $MgSiO_3$ and Mg_2SiO_4 under low and high pressures, in *High Pressure Research in Geophysics,* edited by S. Akimoto and M.H. Manghnani, pp. 511-524, Center for Academic Publications, Tokyo, 1982.

McQueen, R.J., S.P. Marsh, and J.N. Fritz, Hugoniot equation of state of twelve rocks, *J. Geophys. Res., 72,* 4299-5036, 1967.

Meade, C., and R. Jeanloz, Frequency-dependent equation of state of fused silica to 10 GPa, *Phys. Rev. B, 35,* 236-244, 1987.

Nelson, S.A., and I.S.E. Carmichael, Partial molar volumes of oxide components in silicate liquids, *Contrib. Mineral. Petrol., 71,* 117-124, 1979.

Nisbet, E.G., and D. Walker, Komatiites and the structure of the Archaean mantle, *Earth Planet. Sci. Lett., 60,* 105-113, 1982.

Ohtani, E., Generation of komatiite magma and gravitational differentiation in the deep upper mantle, *Earth Planet. Sci. Lett., 67,* 261-272, 1984.

Ohtani, E., F. Taulelle, and C.A. Angell, Al^{3+} coordination changes in liquid aluminosilicates under pressure, *Nature, 314,* 78-81, 1985.

Peselnick, L., R. Meister, and W.H. Wilson, Pressure derivatives of elastic moduli of fused quartz to 10 kb, *J. Phys. Chem. Solids, 28,* 635-639, 1967.

Richet, P., and Y. Bottinga, Anorthite, wollastonite, diopside, cordierite and pyrope: thermodynamics of melting, glass transitions, and properties of the amorphous phases, *Earth Planet. Sci. Lett., 67,* 415-432, 1984.

Rigden, S.M., T.J. Ahrens, and E.M. Stolper, Densities of liquid silicates at high pressures, *Science, 226,* 1071-1074, 1984.

Rigden, S.M., T.J. Ahrens, and E.M. Stolper, Shock compression of molten silicate: Results for a model basaltic composition, *J. Geophys. Res., 93,* 367-382, 1988.

Rivers, M.L., Ultrasonic studies of silicate liquids. Ph.D. dissertation, Univ. of Calif., Berkeley, 1985.

Rivers, M. L., and I. S. E. Carmichael, Ultrasonic studies of silicate melts, *J. Geophys. Res., 92,* 9247-9270, 1987.

Robie, R.A., B.S. Hemingway, and J.R. Fisher, Thermodynamic properties of minerals and related substances at 298.15 K and 1

bar (10^5 pascals) pressure and higher temperatures, *U.S. Geol. Surv. Bull., 1452,* 1978.

Ross, M., and F.J. Rogers, Structure of dense shock-melted alkali halides: Evidence for a continuous pressure-induced structural transformation in the melt, *Phys. Rev. B., 31,* 1463-1468, 1985.

Ruoff, A.L., Linear shock-velocity-particle-velocity relationship, *J. Appl. Phys., 38,* 4976-4980, 1967.

Scarfe, C.M., and E. Takahashi, Melting of garnet peridotite to 13 GPa and the early history of the upper mantle, *Nature, 322,* 354-356, 1986.

Schroeder, J., K.J. Dunn, and F.P. Bundy, Brouillon scattering from amorphous SiO_2 under hydrostatic pressure up to 133 kbar, *Rep. 81CRCD216,* General Electric, Schenectady, N.Y., 1981.

Sharma, S.K., and H.S. Yoder, Structural study of glasses of akermanite, diopside and sodium melilite compositions by Raman spectroscopy, *Year Book Carnegie Inst. Washington, 78,* 526-532, 1979.

Sharma, S.K., B. Simons, and H.S. Yoder, Raman study of anorthite, calcium Tschermak's pyroxene and gehlenite in crystalline and glassy states, *Am. Mineral., 68,* 1113-1125, 1983.

Skinner, B.J., Thermal expansion, Handbook of Physical Constants, edited by S.P. Clark, Jr., *Mem. Geol. Soc. Am., 97,* 75-96, 1966.

Stebbins, J.F., I.S.E. Carmichael, and D.J. Weill, The high-temperature liquid and glass heat contents and heats of fusion of diopside, albite, sanidine and nepheline, *Am. Mineral., 68,* 717-730, 1983.

Stebbins, J.F., I.S.E. Carmichael, and L.K. Moret, Heat capacities and entropies of silicate liquids and glasses, *Contrib. Mineral. Petrol., 86,* 131-148, 1984.

Stolper, E., and T.J. Ahrens, On the nature of pressure-induced coordination changes in silicate melts and glasses, *Geophys. Res. Lett., 14,* 1231-1233, 1987.

Stolper, E., D. Walker, B.H. Hager, and J.F. Hays, Melt segregation from partially molten source regions: The importance of melt density and source region size, *J. Geophys. Res., 86,* 6261-6271, 1981.

Svendsen, B., and T.J. Ahrens, Dynamic compression of diopside and salite to 200 GPa, *Geophys. Res. Lett., 10,* 501-504, 1983.

Taylor, M., and G.E. Brown, Jr., Structure of mineral glasses, I, The feldspar glasses $NaAlSi_3O_8$, $KAlSi_3O_8$, $CaAl_2Si_2O_8$, *Geochim. Cosmochim. Acta, 43,* 61-75, 1979.

Waff, H.S., Pressure-induced coordination changes in magmatic liquids, *Geophys. Res. Lett., 2,* 193-196, 1975.

Weidner, D.J., J.D. Bass, A.E. Ringwood, and W. Sinclair, The single-crystal elastic moduli of stishovite, *J. Geophys. Res., 87,* 4740-4746, 1982.

Williams, D.W., and G.C. Kennedy, Melting curve of diopside to 50 kilobars, *J. Geophys. Res., 74,* 4359-4366, 1969.

T. J. Ahrens and E. M. Stolper, Division of Geological and Planetary Sciences, California Institute of Technology, Pasadena, CA 91125.

S. M. Rigden, Research School of Earth Sciences, Australian National University, Canberra 2601, A.C.T. Australia.

(Received March 14, 1988;
revised December 22, 1988;
accepted January 24, 1989.)